Sum rules and electrodynamics of high-T_c cuprates in the pseudogap state

D. N. Basov, E. J. Singley, and S. V. Dordevic

Department of Physics, University of California, San Diego, La Jolla, California 92093

We explore connections between the electronic density of states (DOS) in a conducting system and the frequency dependence of the scattering rate $1/\tau(\omega)$ inferred from infrared spectroscopy. We show that changes in the DOS upon the development of energy gaps can be reliably tracked through the examination of the $1/\tau(\omega)$ spectra using the sum rules discussed in the text. Applying this analysis to the charge dynamics in high-T_c cuprates, we find radically different trends in the evolution of the DOS in the pseudogap state and in the superconducting state.

I. INTRODUCTION

One of the most enigmatic properties of cuprate high-temperature superconductors is the pseudogap in the spectrum of low-energy excitations developing primarily in weakly doped materials at a temperature T^* well above the superconducting transition T_c.[1] First discovered through experiments probing spin-related behavior, the pseudogap also leads to a characteristic modification of a variety of properties in the charge sector. The microscopic origins of the pseudogap state are still debated. Some aspects of the pseudogap have led to an interpretation of this phenomenon in terms of a "precursor" of the superconducting gap, whereas another school of thought is proposing scenarios based on spin-or charge-density wave fluctuations.[1] In view of the generic character of the pseudogap phenomenon in a large variety of cuprates, it is conceivable that a resolution of the pseudogap puzzles may become an essential step towards elucidating the mechanism of high-T_c superconductivity.

Infrared studies of the electromagnetic response of cuprates are ideally suited for the investigation of the pseudogap and its evolution with temperature and doping. The characteristic features of the pseudogap are distinct in the in plane ($E \| CuO_2$ planes)[2] and in the c-axis ($E \perp CuO_2$ planes) properties.[3–7] In the latter case, the formation of the pseudogap leads to a depletion of the far-IR conductivity with the transfer of the spectral weight to energies above 0.2–0.3 eV. This effect is common for both double-layered materials ($YBa_2Cu_3O_x$, $YBa_2Cu_4O_8$) and for the cuprates with single CuO_2 plane per unit cell $La_{2-x}Sr_xCuO_4$ (La214).[5] The transfer of the spectral weight accounts for the "semiconducting" temperature dependence of the c axis resistivity.

Manifestation of the pseudogap in the $E \| CuO_2$ plane response of cuprates is more subtle in part because the in-plane carrier dynamics is governed by nodal regions of the Fermi surface that remains gapless at all temperatures. The signatures of the pseudogap in the in-plane data are best resolved in the spectra of the frequency-dependent scattering rate,[2,8]

$$\frac{1}{\tau(\omega)} = \frac{\omega_p^2}{4\pi} \text{Re}\left(\frac{1}{\sigma(\omega)}\right), \quad (1)$$

where ω_p is the plasma frequency and $\sigma(\omega) = \sigma_1(\omega) + i\sigma_2(\omega)$ is the complex conductivity.[9] In Eq. (1) ω_p^2

$= 4\pi ne^2/m^*$ is the plasma frequency related to the density of conducting carriers n and inversely proportional to their effective mass m^*.[10] In the underdoped compounds (Fig. 1), the spectra of $1/\tau(\omega)$ are depressed at $T < T^*$ and reveal a characteristic threshold structure at $\Theta \simeq 500 - 600 \, \text{cm}^{-1}$.[2,11] At $\omega < \Theta$, the scattering rate measured at $T < T^*$ increases faster than linear with a crossover to a less rapid (nearly linear) increase at frequencies above the Θ threshold. This behavior is universal and is observed in a large variety of materials.[2,8,11–16] A depression of the scattering rate at low frequencies correlates with transport properties. Indeed, if the threshold structure in $1/\tau(\omega)$ spectra is observed already above T_c, then this behavior is usually accompanied by a faster than linear suppression of the in-plane resistivity at low temperatures.[17,8] As doping progresses to optimal and overdoped, a similar depression of $1/\tau(\omega)$ occurs only at $T \ll T_c$ (right panels in Fig. 1). At $T > T_c$, the scattering-rate spectra in many optimally doped crystals is linear in frequency; this latter behavior correlates with the linear resistivity that one commonly finds at optimal doping.

One possible interpretation of these results is based on phase-space arguments: a partial gap reduces the amount of final states available for scattering of the nodal quasiparticles, thereby leading to a depression of $1/\tau(\omega)$ for energies below the pseudogap. The above argument is corroborated by a close correspondence between the spectra of the scattering rate extracted from IR optics and the form of the electronic self-energy obtained from angular-resolved-photoemission (ARPES) experiments.[18] The phase-space argument also holds for the superconducting gap and thus can qualitatively account for similarity between the $1/\tau(\omega)$ data sets taken in the pseudogap state and at $T \ll T_c$.

In this paper, we attempt to elaborate on the connection between the in-plane dynamics of the charge carriers in cuprates and the gapped character of the density of states (DOS) in these materials. Calculations for a BCS superconductor, as well as experimental examples for relatively simple metallic systems with partially gapped Fermi surface (FS) suggest that the form of the $1/\tau(\omega)$ spectra reproduce the dominant features of the DOS. Therefore, an examination of the temperature dependence of the $1/\tau(\omega)$ spectra may provide an insight into the redistribution of the electronic states upon opening of the pseudogap and superconducting gap in the cuprates. We also discuss the behavior of $1/\tau(\omega)$
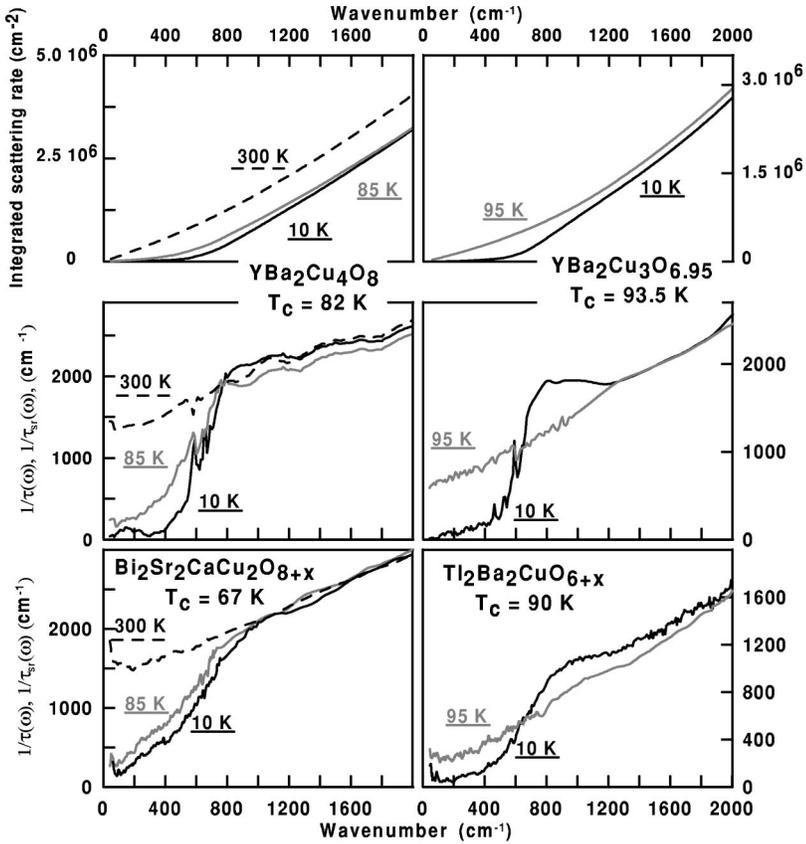
FIG. 1. Middle and bottom panels: the scattering rate $1/\tau(\omega)$ determined for several different cuprates. Within the ω range of this diagram, the spectra of $1/\tau(\omega)$ defined by Eq. (1) and $1/\tau_{sr}(\omega)$ defined by Eq. (7) are indistinguishable from each other. Left panels display data for underdoped materials: $YBa_2Cu_4O_8$ (Y124) (Ref. 2) and $Bi_2Sr_2CaCu_2O_{8+x}$ (Ref. 10). Right panels show data for the optimally doped compounds: $YBa_2Cu_3O_{6.95}$ (YBCO) (Ref. 2) and $Ti_2Ba_2CuO_{6+x}$ (Ref. 11). Solid lines: $T = 10$ K, gray lines: $T \simeq T_c$, dashed lines: $T = 300$ K. The in-plane response of underdoped materials in the pseudogap state is characterized by a depression of $1/\tau(\omega)$ at $\omega < 500-600$ cm^{-1}. In the optimally doped materials, similar depression is observed only in the superconducting state. Top panels show integrated area under the scattering-rate spectra $C(\omega)$ as described in the text.

spectra in different regions of the cuprates phase diagram in the context of sum-rule arguments. This latter analysis unravels marked distinctions between the in-plane electrodynamics in the pseudogap state from what is observed in the superconducting state. We find that the opening of the superconducting gap leads to the expected transfer of the low-energy states from the intragap region to energies above 50–60 meV. The energy scale involved in the formation of the pseudogap appears to be substantially broader. In this latter case, the states removed from the intragap region are not even partially recovered at frequencies as high as 0.2–0.3 eV. Our findings are in agreement with the conclusions based on specific-heat measurements suggesting that the low-energy DOS is depleted in the pseudogap regime.[19] In Sec. II, we examine the generic features of the electromagnetic response of a system with (a partially) gapped Fermi surface. We analyze possible constraints on the behavior of $1/\tau(\omega)$ spectra in such systems imposed by the sum-rule arguments. Section III is dedicated to the implications of the sum-rule analysis for the understanding of the distinctions between the $1/\tau(\omega)$ spectra obtained for several families of cuprates in the superconducting state and in the pseudogap state.

II. $1/\tau(\omega)$ SPECTRA IN A CONDUCTING SYSTEM WITH AN ENERGY GAP

A. Sum-rule arguments

Infrared and optical spectroscopy are powerful techniques for probing energy gaps in solids. For a conducting (metallic) system, determination of the gap is straightforward if the entire FS is affected by the opening of the gap. Examples of such behavior include s-wave superconductors and one-dimensional charge-density wave (CDW) materials.[20] In these systems, the magnitude of the gap E_G can be reliably extracted from the onset of the dissipative part of the conductivity $\sigma_1(\omega)$: at $\omega < E_G$ absorption is prohibited and $\sigma_1(\omega) \simeq 0$. However, in many interesting systems the energy gap affects only a (small) fraction of the Fermi surface. Examples of this latter behavior include d-wave superconductors, heavy-fermion materials, a variety of systems with the so-called correlation gap, etc. Even when the gap is fully developed, these systems remain conducting due to the gapless regions of the FS. This behavior is exemplified in the insets of Fig. 2 and Fig. 3 showing the optical conductivity of a the canonical spin-density wave material Cr and of the heavy-fermion system $YbFe_4Sb_{12}$.[21] Above the temperature of the gap formation, the conductivity of both systems resembles the Drude behavior: a Lorentzian mode centered at $\omega = 0$. The low-temperature spectra of both materials reveal a gaplike structure. Nevertheless, even in the low-T spectra one recognizes a strong Drude-type contribution originating from the gapless regions of the FS.

The gap in $\sigma_1(\omega)$ spectra may become obscured if the width of the Drude component is comparable to, or exceeds, the magnitude of E_G. This is the case in many underdoped cuprates in which the pseudogap leads only to the appearance of weak features in the complex conductivity.[8] The gapped nature of the response appears to be better resolved in the $1/\tau(\omega)$ spectra as can be seen in Figs. 1–3. In all of these systems, the gap is responsible for a characteristic be-
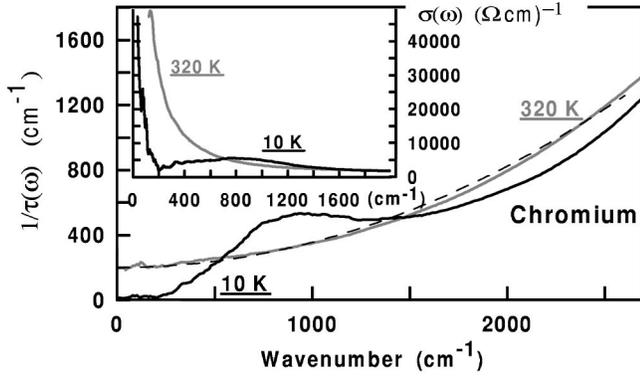
FIG. 2. $1/\tau(\omega)$ spectra for Cr. At $T>T_N$ data follows the form $1/\tau(\omega)\propto\omega^2$ (dashed line) in agreement with the Fermi-liquid theory. At $T=10$ K the SDW gap is fully developed, leading to nontrivial form of the $1/\tau(\omega)$ spectrum described in the text. Inset shows the conductivity spectra.

havior of the scattering rate with a strong depression of $1/\tau(\omega)$ in the intragap region. It follows from Eq. (1) that the $1/\tau(\omega)$ spectra "amplify" the deviations of the experimental conductivity from the Lorentzian form, which is expected if the relaxation phenomena in a solid are dominated by impurity processes with $1/\tau(\omega)=$ const. Such deviations may occur as the result of (strong) interactions in the electronic system: both electron-electron and electron-phonon interactions lead to more complicated functional form of $1/\tau(\omega)$ than a simple constant.[22,23] In the latter case, the scattering rate can be expressed in terms of the integral of the electron-phonon spectral function $\alpha^2 F(\omega)$,

$$\frac{1}{\tau(\omega)} = \frac{2\pi}{\omega} \int_0^\infty d\Omega(\omega-\Omega)\alpha^2 F(\Omega) + \frac{1}{\tau_{\text{imp}}}, \qquad (2)$$

where $1/\tau_{\text{imp}}$ is the impurity scattering. In accord with Eq. (2), the scattering rate may show significant ω dependence at frequencies below the high-energy cutoff of the phonon spectrum. Also, a sharp structure in the electronic density of
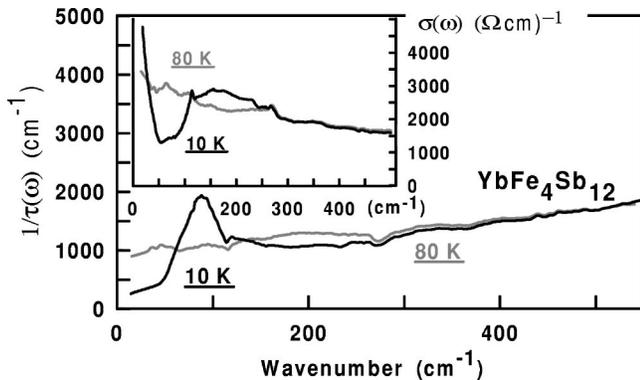
FIG. 3. $1/\tau(\omega)$ spectra for the heavy fermion system YbFe$_4$Sb$_{12}$. Above the coherence temperature ($\simeq 70$ K) the scattering rate is only weakly dependent on frequency and the conductivity spectrum (inset) is Drude-like. At $T=10$ K, the hybridization gap is fully developed, leading to nontrivial form of the $1/\tau(\omega)$ spectrum discussed in the text.
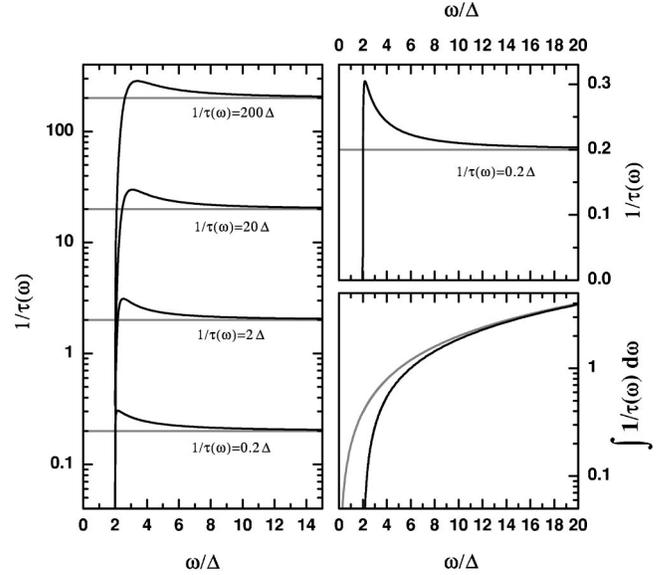
FIG. 4. The frequency dependence of the scattering rate [Eq. (1)] for a BCS superconductor in both the clean and dirty limits (black lines). In the normal state (gray lines), we assumed $1/\tau(\omega)$ = const in accord with the Drude model. Area balance in $1/\tau(\omega)$ spectra holds irrespective of the absolute values of the scattering rate. This attribute of the model spectra is exemplified in the right bottom panel displaying integrals of $1/\tau(\omega)$ at $T=T_c$ and $T=0$ as a function of the cutoff frequency.

states is known to give rise to anomalies in the $1/\tau(\omega)$ spectra.[24] An explicit connection between the density of states and the quasiparticle self-energy has been discussed in the context of the so called mode model by Norman and Ding.[25]

In order to elaborate on connections between the frequency dependence of the $1/\tau(\omega)$ spectra [Eq. (1)] and the essential characteristics of the DOS in conducting systems with a (partial) energy gap, we first turn to the BCS model. We calculated the complex conductivity of a superconductor with an isotropic gap 2Δ both in the clean and dirty limits.[26] We then determined $1/\tau(\omega)$ from Eq. (1). A striking result is that the form of $1/\tau(\omega)$ reproduces the key features of the DOS in a BCS superconductor including the gap feature followed by a sharp peak (Fig. 4). The divergence of the actual DOS at the gap edge is not found in $1/\tau(\omega)$. Also, the peak in $1/\tau(\omega)$ may occur somewhat above the gap energy and its location depends on the strength of impurity scattering. Nevertheless, the overall character of the *single-particle density of states* of a BCS superconductor is reproduced in the $1/\tau(\omega)$ spectra. Depression of $1/\tau(\omega)$ in the intragap region is an obvious consequence of $\sigma_1(\omega)=0$ for $\omega<2\Delta$. However, the appearance of a spike in the calculated dependences above the gap energy is less trivial. This latter behavior, which leads to a resemblance with the DOS, originates from an interplay between the real and imaginary conductivity at frequencies above the gap edge. Similar feature also occurs in $1/\tau(\omega)$ calculated for a d-wave superconductor.[27,28]

An intriguing attribute of the model spectra displayed in Fig. 4 is revealed by the integration of $1/\tau(\omega)$. It appears that the area removed from the intragap region is fully re-

covered due to the overshoot of the spectra at $\omega > 2\Delta$. The reason for the above "sum rule" can be clarified by the following considerations. Expressing $\sigma(\omega)$ in Eq. (1) through the dielectric function $\epsilon_1(\omega) + i\epsilon_2(\omega)$, one finds that

$$\frac{1}{\tau(\omega)} = \frac{\omega_p^2}{\omega} \frac{\epsilon_2}{\epsilon_1^2 + \epsilon_2^2 + 1 - 2\epsilon_1}. \tag{3}$$

The right-hand side (RHS) of Eq. (2) is to be compared with the integrand in the well-known sum rule,[29]

$$\int_0^\infty d\omega \frac{1}{\omega} \frac{\epsilon_2}{\epsilon_1^2 + \epsilon_2^2} = \frac{\pi}{2}. \tag{4}$$

The difference between the RHS of the Eq. (3) and the integrand in the $\pi/2$ sum rule is in the $1 - 2\epsilon_1$ term in the denominator of Eq. (3). It can be easily verified that for any metal $[1 - 2\epsilon_1]$ introduces only a negligibly small correction to the sum of $\epsilon_1^2 + \epsilon_2^2$ at frequencies not too close to the plasma frequency. Therefore, in the regime where $2\Delta \ll \omega_p$ (which is a natural assumption for a BCS superconductor) the spectra of $1/\tau(\omega)$ defined through Eq. (1) are expected to follow a "sum rule" that is most practical for data analysis when written in a differential form,

$$\int_0^{\omega_c} d\omega \left[\frac{1}{\tau^A(\omega)} - \frac{1}{\tau^B(\omega)} \right] \simeq 0. \tag{5}$$

In Eq. (4) indexes A and B refer to different states of the studied system (e.g., normal, pseudogap, superconducting); the cutoff frequency ω_c will be discussed below. According to Eqs. (4), (5) suppression of $1/\tau(\omega)$ in the intragap region ought to be balanced out by the overshoot at $\omega > 2\Delta$. A sum rule for the spectra of $1/\tau(\omega)$ may be expected from the fact that the scattering rate [Eq. (1)] and the frequency-dependent effective mass $m^* = (\omega_p^2/\omega)[\mathrm{Im}(1/\sigma)]$ constitute a legitimate pair of optical constants following Kramers-Kronig (KK) relations and providing a complete description of the electromagnetic response of a solid. Numerous sum rules for other optical constants $[\sigma(\omega), \epsilon(\omega)$, etc.] can all be viewed as consequences of the causality of the response and of the KK integrals in particular. Therefore, a sum rule for $1/\tau(\omega)$ is not an unexpected outcome of basic considerations of the dispersion relations. Recently, Shah and Millis proposed a more formal derivation of the scattering-rate sum rule based on the considerations of Kramers-Kronig relations.[30]

The above arguments based on the $\pi/2$ sum rule [Eq. (4), (5)] provides additional support for the idea of a direct correspondence between the form of $1/\tau(\omega)$ spectra and the density of states in a conducting system with a (partially) gapped Fermi surface. Indeed, the BCS model suggests that the states removed from the intragap region are recovered at energies above the gap. This fundamental conservation is also manifested in the behavior of $1/\tau(\omega)$ depicted in Fig. 4. Moreover, in those situations when $[1 - 2\epsilon_1] \ll [\epsilon_1^2 + \epsilon_2^2]$ the DOS conservation can be quantitatively verified using Eq. (5).

We wish to emphasize upon the distinctions between the information that can be extracted from the sum-rule analysis
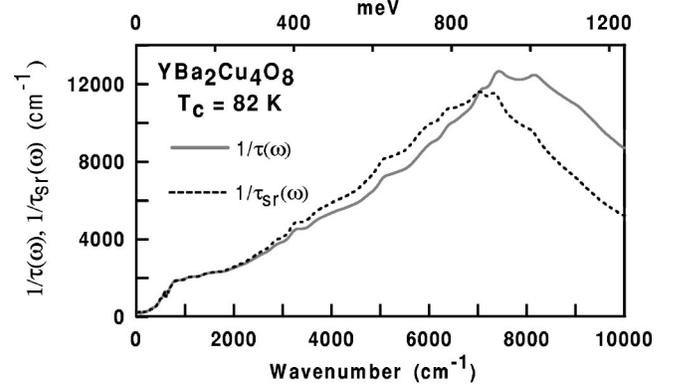
FIG. 5. A comparison of the scattering-rate $1/\tau(\omega)$ spectrum for Y124 crystal obtained at 85 K (gray line) with the $1/\tau_{sr}(\omega)$ spectrum defined by Eq. (7) at the same temperature. The latter quantity exactly follows the $\pi/2$ sum rule and appears to be indistinguishable from $1/\tau(\omega)$ at $\omega < 0.3$ eV.

of the $1/\tau(\omega)$ spectra Eqs. (4), (5) and the oscillator strength f-sum rule for the conductivity

$$\int_0^\infty d\omega \, \sigma_1(\omega) = 4\pi n e^2/m_e, \tag{6}$$

that is commonly used for the examination of the infrared data. The f-sum rule [Eq. (6)] and its numerous modifications provide a useful insight into the redistribution of the *electronic spectral weight* in the studied materials, but often fail to track rearrangements of the *electronic density of states*. Indeed, both superconducting and density-waves gaps lead to an identical form of the density of states,[20] whereas the destination of the spectral weight in the $\sigma_1(\omega)$ is different in these two examples. In a superconductor, this weight is recovered under the δ peak at $\omega = 0$ whereas in the density-wave system the intragap weight is transferred to energies above E_G. The principal advantage of the sum-rule analysis of the $1/\tau(\omega)$ spectra is that this analysis is capable of detecting the changes in the electronic DOS, at least in the case of the two specific examples discussed above.

Before we proceed with the implications of Eqs. (4), (5) it is prudent to discuss potential caveats of the sum rule analysis of the $1/\tau(\omega)$ spectra. As pointed out above, Eq. (5) is not exact because of the $[1 - 2\epsilon_1]$ contribution that we have briefly addressed above. The possible impact of this approximation can be illustrated through a comparison of $1/\tau(\omega)$ spectra with the following quantity:

$$\frac{1}{\tau_{sr}(\omega)} = \frac{\omega_p^2}{\omega} \frac{\epsilon_2}{\epsilon_1^2 + \epsilon_2^2}. \tag{7}$$

It is apparent from Eq. (5) that $1/\tau_{sr}(\omega)$ has the same dimensionality as the scattering rate in Eq. (1) and that $1/\tau_{sr}(\omega)$ *exactly* obeys the $\pi/2$ sum rule. In Fig. 5, we plot both $1/\tau(\omega)$ and $1/\tau_{sr}(\omega)$ dependencies for a Y124 crystal. It is clear from Fig. 5 that for $\omega < 0.3 - 0.4$ eV the frequency dependence of $1/\tau_{sr}(\omega)$ is indistinguishable from that of $1/\tau(\omega)$. Thus, within the frequency range chosen for Figs. 1–3, the spectra of $1/\tau(\omega)$ are identical to $1/\tau_{sr}(\omega)$. At $\omega > 0.5$ eV differences

become noticeable although the general character of both $1/\tau(\omega)$ and $1/\tau_{sr}(\omega)$ spectra still remains the same. Differences are most significant in the vicinity of 1 eV as $\omega \rightarrow \omega_p$. Notably, most of the area, both in $1/\tau(\omega)$ and in $1/\tau_{sr}(\omega)$ spectra (which is of the order of ω_p^2, Ref. 28), is located at energies close to ω_p. This results is important for understanding the temperature dependence of $1/\tau(\omega)$ and $1/\tau_{sr}(\omega)$ from the viewpoint of sum rules Eqs. (4), (5). Indeed, a variety of relaxation mechanisms in solids, including electron-phonon scattering, lead to nearly parallel offsets in both $1/\tau(\omega)$ and $1/\tau_{sr}(\omega)$ spectra throughout the far-IR range[23,8] without noticeable signs of area balance that can be expected from Eq. (5), at least in IR range. However, this temperature dependence affects only a small fraction of the total spectral weight and these minor changes in the $1/\tau_{sr}(\omega)$ at $\omega \ll \omega_p$ are compensated by readjustments in the high-energy part of the spectra.[28] Nevertheless, in the case of the BCS form of the DOS that is realized not only in superconductors but also both in CDW and spin-density wave (SDW) systems as well as in the hybridization-gap compounds, the area balance in the $1/\tau(\omega)$ spectra appears to be fulfilled on the energy scale ω_c comparable to the magnitude of the gap and not to the magnitude of ω_p. This latter circumstance is important for the analysis of the data in the pseudogap state.

B. Experimental results

In Fig. 2 and Fig. 3, we show experimental examples confirming connections between the structure seen in $1/\tau(\omega)$ spectra and the features of the DOS. We studied the response of single crystals of Cr, which is a SDW antiferromagnet with a Neel temperature $T_N = 312$ K.[31] We find that at $T \simeq T_N$ the absolute value of $1/\tau(\omega)$ increases as ω^2 in accord with the Fermi-liquid (FL) theory. At 10 K the SDW gap is fully developed, giving rise to a non-trivial form of the $1/\tau(\omega)$ spectra. The scattering rate is suppressed at $\omega < 500$ cm^{-1}, but then overshoots the 320 K spectrum with a maximum at $\omega \simeq 900$ cm^{-1}. This behavior is similar to the results for the optimally doped cuprates plotted in Fig. 1. The main difference is that cuprates show a linear "background" in $1/\tau(\omega)$ as opposed to the Fermi-liquid ω^2 background seen in the data for Cr.

It is appropriate to compare the frequency dependence of the $1/\tau(\omega, 10K)$ spectrum for Cr with the calculations for a BCS superconductor. This is because the BCS theory is believed to produce an accurate representation of the DOS in a SDW system. While unmistakable similarities are revealed by such a comparison, it is important to keep in mind that in Cr only a part of the Fermi surface is affected by the SDW state.[32] Therefore, the gap in the DOS is incomplete, which may account for a more gradual increase of $1/\tau(\omega)$ in the vicinity of the gap energy compared to theoretical prescriptions in Fig. 4. The detailed sum-rule analysis of the $1/\tau(\omega)$ spectra for Cr is not straightforward because of the vertical offset of the entire curve with decreasing temperature. Such an offset is an expected outcome of the diminishing role of the electron-phonon contribution in $1/\tau(\omega)$.[23,33] Nevertheless, the form of the $1/\tau(\omega, 10K)$ spectrum is suggestive of the DOS transfer from the intragap region to the overshoot. In-

tegration of the two spectra with the cutoff 1500 cm^{-1} indicates that the balance in $1/\tau(\omega)$ measured for Cr is fulfilled with an accuracy of 10%.

In Fig. 3, we show the data for a heavy-fermion material YbFe$_4$Sb$_{12}$. The origin of the energy gap in heavy-fermion compounds is believed to be in hybridization between the f level and the conduction band.[34,21] The gap usually develops below the so-called coherence temperature T_{coh}. The formation of the gaps leads to a sharp peak in the density of states as discussed in Ref. 35. The conductivity spectrum obtained for YbFe$_4$Sb$_{12}$ at $T > T_{coh}$ shows a Drude-like behavior corresponding to nearly frequency-independent spectrum of $1/\tau(\omega)$. At $T < T_{coh}$, the gap is clearly visible in the $1/\tau(\omega)$ data: The magnitude of $1/\tau(\omega)$ is suppressed in the intragap region. This is followed by a sharp peak at $\omega > E_G$, so that the low-temperature spectrum overshoots the curve obtained at $T > T_{coh}$. The area balance in the $1/\tau(\omega)$ expected from Eqs. (4), (5) is confirmed with an accuracy better than 7% through an explicit integration of these spectra up to 400 cm^{-1}.

It is apparent from Figs. 2–4 that the spectra of $1/\tau(\omega)$ capture the gross characteristics of the density of states in a conducting system, especially in those situations when the DOS is partially or completely gapped. This conclusion also holds for CDW materials such as TaSe$_2$[36] and BaRuO$_5$.[37] We emphasize again, that in those cases when a (partial) gap in the DOS is well documented (BCS, CDW, hybridization) the area balance of in the $1/\tau(\omega)$ spectra is fulfilled on the energy scale ω_c comparable to E_G and *not* to the scale of the plasma frequency.

III. SUPERCONDUCTING GAP AND PSEUDOGAP FROM THE VIEWPOINT OF THE SCATTERING RATE SUM RULES

We now return to the data for cuprates, focusing on the implications of Eqs. (4), (5) for the understanding of the charge response across the phase diagram. As pointed out above, the dominant features of the $1/\tau(\omega)$ spectra obtained for underdoped crystals in the pseudogap state are similar to those seen at $T \ll T_c$ in the optimally doped samples. On closer examination one finds differences as well. Suppression of $1/\tau(\omega)$ at $\omega < \Theta$ in the pseudogap state *does not* lead to the development of an overshoot between the spectra measured at $T \ll T^*$ and $T > T^*$. The data for the optimally doped crystals taken at $T \ll T_c$ and $T \simeq T_c$ does reveal an overshoot at $\omega \simeq 800$ cm^{-1}.[38] In the latter case, the area under the overshoot is balanced out by the reduction of $1/\tau(\omega)$ at low energies with an accuracy better than 10% in Tl$_2$Ba$_2$CuO$_6$ crystal and about 15% in the YBa$_2$Cu$_3$O$_{6.95}$ sample.[39] Both the area balance and the form of the $1/\tau(\omega)$ spectra for the optimally doped system are in accord with the notion of the transfer of states from the intragap region to a peak at $\omega > \Theta$. This behavior can be naturally attributed to the opening of the superconducting energy gap. Although, the absolute values of the optical constants for the underdoped compounds are also in the regime when Eq. (5) ought to be satisfied, the data gives no indications even for a partial recovery of the area associated with the far-IR depression of

$1/\tau(\omega)$ in the pseudogap state. Notably, additional suppression of the scattering rate at $T<T_c$ in Y124 crystal occurs in accord with the Eq. (5). This is illustrated in the top panels of Fig. 1 presenting the integrated area under the $1/\tau(\omega)$ spectra: $C(\omega)=\int_0^\omega d\omega'[1/\tau(\omega')]$.

The above results show that the spectra taken above and below T^* "violate" Eqs. (4), (5) within the frequency range of Fig. 1 whereas no similar violation is detected in the data at $T<T_c$ (neither for optimally doped nor for underdoped samples). Therefore, the sum-rule analysis of $1/\tau(\omega)$ signifies the differences in the changes of the low-energy DOS in the pseudogap state from the changes associated with superconductivity. Essentially, the analysis described above indicates that the states removed from $\omega<\Theta$ at $T<T^*$ disappear from the energy interval reliably sampled in our experiments (0.5 eV). This result is in accord with tunneling studies of the temperature dependence of the electronic DOS in underdoped cuprates.[40] Indeed, data obtained at $T\ll T_c$ reveals a transfer of the electronic states from the intragap region in the quasiparticle peaks just above the gap. On the contrary, the formation of the pseudogap only leads to a depletion of DOS without visible traces of recovery of $D(\omega)$, at least at $\hbar\omega<0.1$ eV. Specific-heat measurements are also in accord with our findings since these experiments suggest a reduction of the DOS in the pseudogap state within the energy window accessible to thermodynamic probes ($\simeq500$ K).[19] Another indication of an energy scale extending beyond 0.1–0.5 eV that is involved in the pseudogap-state response is provided by the IR studies of the interlayer c-axis conductivity $\sigma_c(\omega)$. Nonconservation of the low-energy spectral weight $N_{eff}(\omega)=\int_0^\omega d\omega'\,\sigma_c(\omega')$ for $\omega<0.2$–0.4 eV is inferred from the oscillator strength sum rule,[3,4,7,41] these c-axis results parallel our findings deduced from the examination of the in-plane scattering rate using Eqs. (4), (5). Thus, one can conclude that both spectroscopic and thermodynamic studies of cuprates reveal anomalous changes of the DOS in the pseudogap state, distinct from the effects associated with superconductivity. Hence, these results argue against a common origin of the pseudogap state and superconducting state.

Further support for the distinct genesis of the pseudogap and of superconducting gap is provided by the data for $La_{2-x}Sr_xCuO_4$ (La214) and $Nd_{2-x}Ce_xCuO_4$ (Nd214) materials. The scattering-rate analysis of the in-plane response of these systems reveals a characteristic threshold structure at $\Theta\simeq500$–600 cm^{-1}.[14,15] In the double- or triple-layered materials, the development of superconducting gap occurs approximately at the same energy as the pseudogap structure. However, in La214 and Nd214 compounds, the signatures attributable to superconductivity are confined to energies below 40–50 cm^{-1} (Refs. 15, 42) whereas the pseudogap feature is essentially identical to what is seen in the double-layered compounds with $\Theta\simeq500$–600 cm^{-1}. It is difficult to account for the difference by more than one order of magnitude between the energy scales associated with the pseudogap and with superconductivity if both effects have the same origin.

The formation of the pseudogap in cuprates is commonly discussed in the context of density-wave ideas. Our analysis, in conjunction with the data for a canonical SDW system such as Cr, argues against this point of view as well. Experimental results obtained both for SDW and CDW systems are in accord with quite conventional transfer of the intragap states to the energy region right above the gap. Therefore, both spin and charge-density waves are unable to account for the experimental situation of the pseudogap state in high-T_c cuprates. Nonconservation of the low-energy DOS in the pseudogap regime has been recently discussed by Varma.[43]

In conclusion, the sum-rule analysis of the optical constants based on Eqs. (4)–(5) argues against the decisive role of both superconducting and density-wave fluctuations in the formation of the pseudogap. We emphasize that the scale associated with the spectroscopic signatures of the pseudogap dramatically exceeds the characteristic temperature T^* as well as the energy of antiferromagnetic exchange J (typically 0.15 eV) and is of the order of the energies of the interband transitions in cuprates. Such a disproportion between ω and T scales may signal the relevance of many-body effects to the formation of the pseudogap state. A similar mismatch between temperature and energy scales is know to occur in bilayer quantum-Hall systems and is ascribed to many-body interactions.[44] The Mott ransitiont in V_2O_3 crystals is yet another example of a remarkable difference between k_BT and $\hbar\omega$ scales in an interacting system.[45]

[1] T. Timusk and B. Statt, Rep. Prog. Phys. **62**, 61 (1999); J. Orenstein and A. J. Millis, Science **288**, 468 (2000).

[2] D. N. Basov, R. Liang, B. Dabrowski, D. A. Bonn, W. N. Hardy, and T. Timusk, Phys. Rev. Lett. **77**, 4090 (1996).

[3] C. C. Homes, T. Timusk, R. Liang, D. A. Bonn, and W. N. Hardy, Phys. Rev. Lett. **71**, 1645 (1993).

[4] D. N. Basov, T. Timusk, B. Dabrowski, and J. D. Jorgensen, Phys. Rev. B **50**, 3511 (1994).

[5] D. N. Basov, H. A. Mook, B. Dabrowski, and T. Timusk, Phys. Rev. B **52**, R13 141 (1995).

[6] S. Tajima, J. Schtzmann, S. Miyamoto, L. Terasaki, Y. Sato, and R. Hauff, Phys. Rev. B **55**, 6051 (1997).

[7] C. Bernhard, D. Munzar, A. Wittlin, W. Knig, A. Golnik, C. T. Lin, M. Klser, Th. Wolf, G. Müller-Vogt, and M. Cardona, Phys. Rev. B **59**, 6631 (1999).

[8] A. V. Puchkov, D. N. Basov, and T. Timusk, J. Phys.: Condens. Matter **8**, 10 (1996).

[9] The conductivity spectra are usually obtained from Kramers-Kronig (KK) analysis of the raw reflectance data. Extrapolations to high and low energies required for the KK transformations

have only a minor impact on the $1/\tau(\omega)$ spectra in the frequency region where the actual data exist. For a review see, for example, Ref. 8.

[10] Experimentally, ω_p is usually determined from integrating the conductivity up to a cutoff frequency 1.75–2 eV: $\omega_p = \int d\omega \, \sigma_1(\omega)$; this choice of the cutoff roughly corresponds to the onset of the interband contribution to $\sigma_1(\omega)$. For all materials discussed in this work, the plasma frequency determined in this way is found to be temperature independent with 5–10 % accuracy.

[11] A. V. Puchkov, P. Fournier, D. N. Basov, T. Timusk, A. Kapitulnik, and N. N. Kolesnikov, Phys. Rev. Lett. **77**, 3212 (1996).

[12] A. V. Puchkov, T. Timusk, S. Doyle, and A. M. Hermann, Phys. Rev. B **51**, 3312 (1995).

[13] J. J. McGuire, M. Windt, T. Startseva, T. Timusk, D. Colson, and V. Viallet-Guillen, Phys. Rev. B **62**, 8711 (2000).

[14] T. Startseva, T. Timusk, A. V. Puchkov, D. N. Basov, H. A. Mook, M. Okuya, T. Kimura, and K. Kishio, Phys. Rev. B **59**, 7184 (1999).

[15] E. J. Singley, D. N. Basov, K. Kurahashi, T. Uefuji, and K. Yamada, Phys. Rev. B **64**, 224503 (2001).

[16] A threshold structure in the spectra of $1/\tau(\omega)$ corresponds to a "kink" in the dispersion dependence probed in the ARPES measurements. Recently, an observation of this feature in several different families of cuprates has been reported by A. Lanzara, P. V. Bogdanov, X. J. Zhou, S. A. Kellar, D. L. Feng, E. D. Lu, T. Yoshida, H. Elsaki, A. Fujimori, K. Kishio, J.-I. Shimoyama, T. Noda, S. Uchida, Z. Hussain, and Z.-X. Shen, Nature (London) **412**, 510 (2001).

[17] K. Takenaka, H. Takagi, and S. Uchida, Phys. Rev. B **50**, 6534 (1994).

[18] A. Kaminski, J. Mesot, H. Fretwell, J. C. Campuzano, M. R. Norman, M. Randeria, H. Ding, T. Sato, T. Takahashi, T. Mochiku, K. Kadowaki, and H. Hoechst, Phys. Rev. Lett. **84**, 1788 (2000); P. D. Johnson, T. Valla, A. V. Fedorov, Z. Yusof, B. O. Wells, Q. Li, A. R. Moodenbaugh, G. D. Gu, N. Koshizuka, C. Kendziora, S. Jian, and D. G. Hinks, *ibid.* **87**, 177007 (2001).

[19] J. W. Loram, K. A. Mirza, J. R. Cooper, and W. Y. Liang, Phys. Rev. Lett. **71**, 1740 (1993).

[20] G. Gruner, *Density Waves in Solids* (Addison-Wesley, Reading, MA, 1994).

[21] S. V. Dordevic, D. N. Basov, N. R. Dilley, E. D. Bauer, and M. B. Maple, Phys. Rev. Lett. **86**, 684 (2001).

[22] P. B. Allen, Phys. Rev. B **3**, 305 (1971).

[23] S. V. Shulga, O. V. Dolgov, and E. G. Maksimov, Physica C **178**, 266 (1991).

[24] W. Pickett and P. B. Allen, Solid State Commun. **12**, 677 (1973).

[25] M. R. Norman and H. Ding, Phys. Rev. B **57**, 11 089 (1998).

[26] L. Leplae, Phys. Rev. B **27**, 1911 (1983).

[27] T. Dahm and L. Tewordt, Phys. Rev. Lett. **74**, 793 (1995); A. Abanov and A. Chubukov, cond-mat/0112085 (unpublished).

[28] F. Marsiglio, J. P. Carbotte, and E. Schachinger, cond-mat/0110021 (unpublished); also J. P. Carbotte (private communications).

[29] D. Pines and P. Nozihres, *The Theory of Quantum Liquids* (Benjamin, New York, 1966); G. Mahan, *Many-Particle Physics* (Plenum, New York, 1980).

[30] N. Shah and A. J. Millis, Phys. Rev. B **64**, 174506 (2001).

[31] We measured the reflectance of mechanically polished crystals in the frequency region 30–25 000 cm^{-1}. Reflectance results were supplemented with the ellipsometry data at frequencies up to 38 000 cm^{-1}. Optical constants were determined from reflectance using KK analysis by taking into account phase determined through ellipsometry.

[32] E. Fawcett, Rev. Mod. Phys. **60**, 209 (1988).

[33] For calculations of $1/\tau(\omega,T)$ spectra within a model of strong electron-phonon coupling see, for example, Fig. 5 in Ref. 8.

[34] L. Degiorgi, Rev. Mod. Phys. **71**, 687 (1999).

[35] G. Travaglini and P. Wachter, Phys. Rev. B **29**, 893 (1984).

[36] T. Valla, A. V. Fedorov, P. D. Johnson, J. Xue, K. E. Smith, and F. J. DiSalvo, Phys. Rev. Lett. **85**, 4759 (2000).

[37] Y. S. Lee, J. S. Lee, K. W. Kim, T. W. Noh, J. Yu, E. J. Choi, G. Cao, and J. E. Crow, Europhys. Lett. **55**, 280 (2001). Scattering-rate analysis is not reported in this paper; $1/\tau(\omega)$ results were communicated by Y. S. Lee.

[38] Because the overshoot in the $1/\tau(\omega)$ spectra is related to the quasiparticle peak (QP) in the DOS, several factors may affect the prominence of this feature in the IR data. For instance, impurities are known to suppress the QP peak as shown for Bi2212 compounds through tunneling measurements. S. H. Pan, J. P. O'Neal, R. L. Badzey, C. Chamon, H. Ding, J. R. Engelbrecht, Z. Wang, H. Eisaki, S. Uchida, A. K. Gupta, K. W. Ng, E. W. Hudson, K. M. Lang, and J. C. Davis, Nature (London) **413**, 282 (2001).

[39] The area balance in the $1/\tau(\omega)$ spectra for YBCO and Tl2201 compounds is expected from Eqs. (3)–(4) because the contribution of $1 - 2\epsilon_1$ term within the frequency range presented in Fig. 1 is negligibly small for either of the above superconductors.

[40] Ch. Renner, B. Revaz, J.-Y. Genond, K. Kadowaki, and O. Fischer, Phys. Rev. Lett. **80**, 149 (1998); N. Miyakawa, J. F. Zasadzinski, L. Ozyuzer, P. Guptasarma, D. G. Hinks, C. Kendziora, and K. E. Gray, *ibid.* **83**, 1018 (1999); V. M. Krasnov, A. Yurgens, D. Winkler, P. Delsing, and T. Claeson, *ibid.* **84**, 5860 (2000).

[41] D. N. Basov, S. I. Woods, A. S. Katz, E. J. Singley, R. C. Dynes, M. Xu, D. G. Hinks, C. C. Homes, and M. Strongin, Science **283**, 49 (1999); M. Güninger, D. van der Mare, A. A. Tsvetkov, and A. Erb, Phys. Rev. Lett. **84**, 1575 (2000).

[42] F. Gao, D. B. Romero, D. B. Tanner, J. Talvacchio, and M. G. Forrester, Phys. Rev. B **47**, 1036 (1993); H. S. Somal, B. J. Feenstra, J. Schützmann, J. H. Kim, Z. H. Barber, V. H. M. Duijn, N. T. Hien, A. A. Menovsky, M. Palumbo, and D. van der Marel, Phys. Rev. Lett. **76**, 1525 (1996); M. Dumm, D. N. Basov, and Y. Ando (unpublished); T. Sato, T. Kamiyama, T. Takahashi, K. Kurahashi, and K. Yamada, Science **291**, 1517 (2001); N. P. Armitage, D. H. Lu, D. L. Feng, C. Kim, A. Damascelli, K. M. Shen, F. Ronning, Z.-X. Shen, Y. Onose, Y. Taguchi, and Y. Tokura, Phys. Rev. Lett. **86**, 1126 (2001).

[43] C. M. Varma, Phys. Rev. Lett. **83**, 3538 (1999).

[44] T. S. Lay, Y. W. Suen, H. C. Manoharan, X. Ying, M. B. Santos, and M. Shayegan, Phys. Rev. B **50**, 17 725 (1994); S. Q. Murphy, J. P. Eisenstein, G. S. Boebinger, L. N. Pfeiffer, and K. W. West, Phys. Rev. Lett. **72**, 728 (1994).

[45] M. J. Rozenberg, G. Kothar, H. Kajueter, G. A. Thomas, D. H. Rapkine, J. M. Honig, and P. Metcalf, Phys. Rev. Lett. **75**, 105 (1995).